

# EGFR-targeting Peptide Conjugated pH-sensitive Micelles as a Potential Drug Carrier for Photodynamic Detection and Therapy of Cancer

Cheng-Liang Peng<sup>1</sup>, Yuan-I Chen<sup>2</sup>, Ying-Hsia Shih<sup>1</sup>, Tsai-Yueh Luo<sup>1</sup> and Ming-Jium Shieh<sup>2</sup>

<sup>1</sup>Isotope Application Division, Institute of Nuclear Energy Research, Taoyuan, Taiwan

<sup>2</sup>Institute of Biomedical Engineering, College of Medicine, National Taiwan University, Taipei, Taiwan

**Keywords:** Thermosensitive, Photothermal Therapy, Chemotherapy, Micelle, Control Release, Synergistic Effect.

**Abstract:** Multifunctional theranostics have recently been intensively explored to optimize the efficacy and safety. Herein, we report multifunctional micelle that constructed from graft copolymer PEGMA-co-PDPA and diblock copolymer mPEG-b-PCL as the carrier of hydrophobic photosensitizer, chlorin e6 (Ce6) for simultaneous fluorescence imaging and photodynamic therapy. The functional inner core of PEGMA-co-PDPA exhibited pH stimulate to accelerate drug release under slightly acidic microenvironments of tumors and the outer shell of micelles with epidermal growth factor receptor (EGFR)-targeting GE11 peptides for active targeting of EGFR-overexpressing cancer cells. The results demonstrate that GE11-conjugated chlorin e6-loaded micelles (GE11-Ce6-micelles) with particle size around 100 nm and the micelles had well defined core shell structure which was evaluated by TEM. In the in vitro cellular uptake studies, GE11-Ce6-micelles exhibited a higher amount of intracellular uptake of chlorin e6 in HCT116 cancer cells (EGFR high expression) via receptor-mediated endocytosis, in contrast with the time-dependent passive uptake of the non-targeted Ce6-micelles, thereby providing a effective photocytotoxic effect on the HCT116 cancer cells. In vivo study revealed that GE11-Ce6-micelles exhibited tumor targeting for photodynamic detection and excellent inhibition on tumor growth after irradiation, indicating that GE11-Ce6-micelles could be successfully applied to the effective fluorescence imaging and photodynamic therapy of cancer.

## 1 INTRODUCTION

Photodynamic therapy (PDT) is a novel treatment for several diseases including age-related macular degeneration, periodontitis and malignant cancers (Schmidt-Erfurth and Hasan, 2000). PDT is based on a photochemical reactions that could produces localized tissue damage. The activation of photosensitizers in the target tissues by suitable wavelengths of light would lead to generations of reactive oxygen species (ROS) to destroy cancer cells. Important advantages of PDT over other therapies include minimal invasiveness, repeated PDT applicability at the same site, high therapeutic efficacy, and less side effects in comparison with other treatments of cancer (Wang et al., 2014a).

Chlorin e6 (Ce6) is a promising photosensitizer for PDT with an excitation wavelength at 660 nm. Chlorin e6 exhibits advantageous photophysical properties including having long lifetimes in its

photoexcited triplet states and high absorption in the red spectral region that could penetrate tissues deeper (Wang et al., 2014b). Despite these significant advantages, Chlorin e6 has poor solubility in aqueous media and nonspecific biodistribution with low tumor-targeting efficacy, which could cause drug loss or photosensitivity in healthy tissues (Zhang et al., 2003).

The slight acidic microenvironment of solid tumor is resulted from their high metabolic rate via anaerobic glycolysis that causes accumulation of lactic acid and carbon dioxide. Electrical and chemical probes show that the pH of the microenvironment is around 5.8 - 7.2, which is lower than the physiological pH of 7.4 (Shen et al., 2008).

To further enhance drug accumulation in tumor sites while minimizing drug concentration in other sites, nanoparticles are now being conjugated with targeting ligands, such as antibodies, proteins,

aptamers, and peptides (Lee et al., 2013). Peptides are small molecules with specific receptor binding, low immune response induction, and high stability *in vivo*. These characteristics of peptides make them better tumor targeting ligands. The epidermal growth factor receptor (EGFR) is a cell surface receptor that is highly expressed in human epithelial cancer cells, including breast, lung, ovarian, and colon cancers (Arteaga, 2002).

In this study, the structure and pH sensitivity of multifunctional micelles were determined and characterized. The cellular uptake efficiency was evaluated in HCT116 cells (high EGFR expression) and SW620 cells (low EGFR expression). At last, the *in vivo* tumor-targeted PDT efficacy and imaging were evaluated in tumor-bearing mice. The pH-sensitive micelle conjugated with GE11 peptide is expected to accelerate drug release under slightly acidic microenvironments of tumors and be internalized via EGFR-mediated endocytosis (scheme 1). The goal of this study is to develop a drug delivery system with enhanced tumor targeting for cancer therapy.

## 2 EXPERIMENTAL SECTION

### 2.1 Synthesis of PEGMA-co-PDPA, mPEG-PCL, and mal-PEG-PCL

The pH-sensitive copolymer, PEGMA-co-PDPA (poly(ethylene glycol) methacrylate-co- poly(2-(diisopropylamino)ethyl methacrylate) was synthesized by free radical polymerization as described previously (Peng et al., 2010). Briefly, PEGMA (0.25 g) and DPA (0.5 g) were added to a flask equipped with a magnetic stirrer and 5 ml THF. The AIBN initiator (9.25 mg) was added to the mixture and the solution was heated at 70 °C for 24 h in an atmosphere of nitrogen. Unreacted monomers were removed by dialysis against water for 3 days and the polymer fraction was lyophilized. Copolymer compositions were determined with FT-NMR at 500 MHz using chloroform-d (CDCl<sub>3</sub>) as the solvent.

### 2.2 Preparation of Chlorin E6-Loaded Micelles

The blank micelles were prepared by dialysis method (Chaw et al., 2004). In brief, different weights (0~5mg) of PEGMA-co-PDPA and mPEG-PCL were dissolved completely in 0.1N HCL and then dialysis of base solution for 1 day. Chlorin e6-

loaded micelles (Ce6-micelles) were prepared via the cosolvent evaporation method (Peng et al., 2008a). Briefly, 10 mg of PEGMA-co-PDPA, 10mg of PEG-PCL, and 2mg of mal-PEG-PCL were dissolved in 0.5 ml THF with Chlorin e6 (1~4mg) and then added to 5 ml of PBS with stirring at 550 rpm. The organic solvent was evaporated while being stirred overnight and the remaining portion was filtered through a 0.22 μm pore size Millex GS filter to remove non-incorporated drug crystals.

### 2.3 Preparation of GE11-conjugated Micelles

EGFR specific peptide (GE11, sequence: YHWYGYTPQNVI-GGGGC) was used to establish active targeted micelles (Li et al., 2005). The sequence of "GGGG" as a spacer while the carboxyl terminal cysteine of the peptide conjugated with the maleimide of the micelles (Milane et al., 2010). The conjugation of GE11 was then just performed by mixture of GE11 and maleimide containing micelles with different molar ratio at 4 °C overnight, as described previously (Olivier et al., 2002). The unconjugated GE11 peptide was separated by passing through PD-10 desalting column (GE Healthcare, Uppsala, Sweden).

### 2.4 Characterization of Chlorin E6-Loaded Micelles

The mean diameter and PDI of micelles were determined using a Zetasizer Nano ZS90 apparatus (Malvern Instruments, Worcestershire, UK). The size and morphology of micelles were ascertained by transmission electron microscopy (TEM) using a model H-7650 microscope (Hitachi, Tokyo, Japan). To prepare a TEM sample, a drop of sample solution was placed on a 200-mesh carbon-coated copper grid and then the excess solution was removed with filter paper.

The pH sensitivity of micelle was recorded through size and zeta potential measurements by dynamic light scattering at various pH values of PBS.

### 2.5 In Vivo Fluorescence Imaging

To observe biodistribution of Chlorin e6, female BALB/c athymic (nut/nut) mice (5-6 weeks old) were purchased from the National Laboratory Animal Center (Taipei, Taiwan). HCT-116 cells (1×10<sup>6</sup>) and SW620 cells (1×10<sup>6</sup>) were inoculated subcutaneously on the right and left flanks of nude

mice, respectively. When the tumors reached a volume of 150 to 200 mm<sup>3</sup>, mice received an intravenous injection of Ce6-micelles or GE11-Ce6-micelles (equivalent to 5 mg/kg of Ce6). The *in vivo* biodistribution of Ce6 were imaged at 3 and 24 after intravenous injection using an IVIS imaging system (Xenogen, Alameda, CA, USA). The tumor-bearing mice were sacrificed 24 h post-injection, major organs and tumors were excised for isolated organ imaging to estimate the tissue distribution of Ce6-micelles or GE11-Ce6-micelles.

## 2.6 In Vivo Photodynamic Therapy

HCT116 cells ( $1 \times 10^6$  cells) were implanted subcutaneously into the right flanks of mice. When tumors grew to approximately 150-200 mm<sup>3</sup> in volume, 200-500  $\mu$ l of PBS containing Ce6-micelles or GE11-Ce6-micelles (equivalent to 5 mg/kg of Ce6) were injected via tail vein ( $n = 4$  per each group). At 24 h after injection, tumor tissues were irradiated by 670 nm diode laser (634 mW/cm<sup>2</sup>) for 10 min.

## 3 RESULTS AND DISCUSSION

### 3.1 Synthesis and Characterization of Polymers

In this study, the pH-responsive micelles assembled from mixture of graft copolymer PEGMA-co-PDPA and diblock copolymer mPEG-PCL were developed to control drug delivery and enhance the antitumor efficacy of photodynamic therapy. Synthesis of PEGMA-co-PDPA and mPEG-b-PCL were carried out as shown in Figure 1. The potentiometric measurements was performed to determine the pK<sub>a</sub> of the PEGMA-co-PDPA copolymers, each of the DPA-based copolymers presented a sharp protonation transition in the pH range 6.0 to 7.0. According to the pH transition of PEGMA-co-PDPA, the pH-responsive micelles can deliver successfully the anticancer drugs to target tumor tissue but minimize the drug release at normal tissues. The diblock copolymer, mPEG-PCL were synthesized by ring-opening polymerization (Peng et al., 2009).

The micelles ranged from 91.05 to 142.37 nm in size with various polydispersity indices (Table 1).

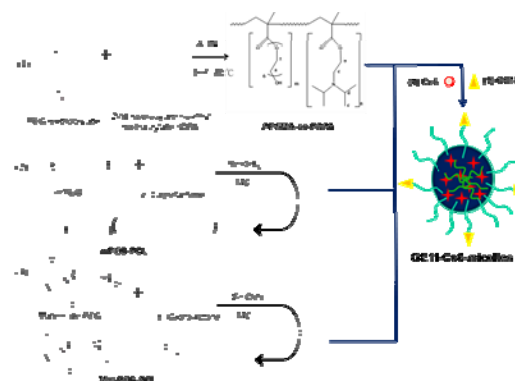


Figure 1: Schematic diagram illustrates the fabrication of GE11-Ce6-micelles.

### 3.2 Characterization of Chlorin E6-Loaded Micelles

Chlorin e6 as a photosensitizer was efficiently encapsulated into the pH-responsive micelles, due to the hydrophobic interactions between chlorin e6 and hydrophobic group as DPA or PCL of micelles. Table 1 lists the results of the loading efficiency, drug contents, and sizes of the chlorin e6 loaded pH responsive micelles. After incorporating various amounts of chlorin e6, all of the samples had a narrow PDI from 0.109-0.154 and ranged in size from 96.6-103.1 nm. Chlorin e6-loaded micelles with a D/P ratio of 1/10 were used and the encapsulation efficiency was 86.25%. When the micelles with a D/P ratio of 1/5 or 1/20 were employed, the encapsulation efficiency was lower

Table 1: Characteristics of micelles.

Sample	D/P ratio	encapsulation efficiency (%)	drug content (%)	Mean size /nm(PDI)
micelles	-	-	-	91.1 (0.239)
Ce6-micelles	1/5	75.52	12.09	96.6 (0.109)
Ce6-micelles	1/10	86.25	7.82	96.7 (0.125)
Ce6-micelles	1/20	74.35	3.54	103.1 (0.154)
Mal-micelles	-	-	-	105.7 (0.222)
Ce6-Mal-micelles	1/10	85.9	7.81	110.0 (0.184)
GE11-Ce6-micelles	1/10	78.8	7.16	105.1 (0.293)

than those with a D/P ratio of 1/10. Figure 2 showed the morphology of the nanoparticles with or without chlorin e6 as observed by TEM. The images indicated that micelles with different conditions were uniform, spherical, and the particle size agreed with the results measured by dynamic light scattering (DLS). Absorbance and fluorescence spectra of chlorin e6-loaded mixed micelles (Ce6-micelles), and GE11-conjugated chlorin e6-loaded mixed micelles (GE11-Ce6-micelles) revealed that free chlorin e6 exhibited a relatively broad and weak fluorescence, while the fluorescence of chlorin e6-loaded mixed micelles was strong and reached a maximum at 670 nm as show in Figure 3.

### 3.3 Cellular Uptake and Localization of Chlorin E6-Loaded Micelles

Subcellular localization of EGFR-targeted GE11-Ce6-micelles or non-targeted Ce6-micelles were evaluated by using fluorescence microscopy as shown in Figure 4. After 5 h incubation, the GE11-Ce6-micelles were rapidly taken up by the HCT116 cells, as that could be observed from the green fluorescence of FITC-labeled micelles accumulated in cells. Intracellular drug release by targeted micelles and non-targeted micelles could be projected by red fluorescence of chlorin e6.

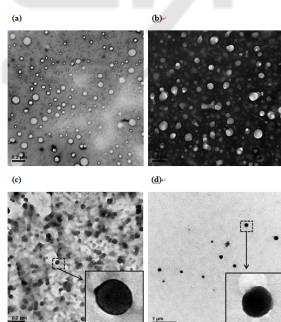


Figure 2: Transmission electron micrographs images of (a) PEGMA-co-DPA micelles, (b) mixed micelles, (c) chlorin e6 loaded mixed micelles (Ce6-micelles), and (d) chlorin e6 loaded GE11-conjugated mixed micelles (GE11-Ce6-micelles).

The fluorescence of GE11-Ce6-micelles significantly accumulated in the cytoplasm but not in the nucleus. Furthermore, the most fluorescence of chlorin e6 in HCT116 cells were colocalized with the fluorescence of micelles. However, the fluorescence intensity of chlorin e6 in HCT116 cells remarkably decreased when cells treated with GE11-Ce6-micelles and excess amount of free GE11 peptides, indicated that the specific uptake of GE11-Ce6-micelles into tumor cells through EGFR-

mediated endocytosis.

### 3.4 In Vivo Fluorescence Imaging

To compare the in vivo biodistribution of EGFR-targeted GE11-Ce6-micelles or non-targeted Ce6-micelles (equivalent to 5mg/kg of chlorin e6) was injected intravenously into HCT116 (high expression EGFR) and SW620 (low expression EGFR) tumor-bearing mice. The in vivo biodistribution of chlorin e6 could be directly monitored by non-invasive and real-time fluorescence imaging of the whole body, because chlorin e6 can emit strong near infrared (NIR) fluorescence for efficient tracking (Koo et al., 2010).

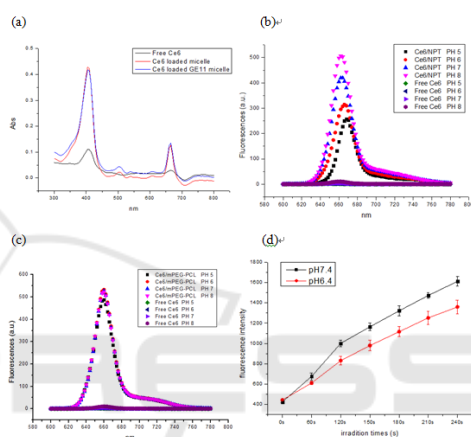


Figure 3: (a) Absorbance spectra of free chlorin e6 (Ce6), chlorin e6-loaded mixed micelles (Ce6-micelles), and GE11-conjugated chlorin e6-loaded mixed micelles (GE11-Ce6-micelles) (b) fluorescence spectra of GE11-Ce6-mixed micelles in difference pH values of buffers, (c) fluorescence spectra of chlorin e6-loaded mPEG-b-PCL micelles in difference pH values of buffers (equivalent to 2 µg/ml of chlorin e6). The fluorescence spectra were measured with an excitation of 403 nm and emissions in the 600–800 nm range. (d) Singlet oxygen generation of GE11-Ce6-micelles in various pH Tris buffer solutions.

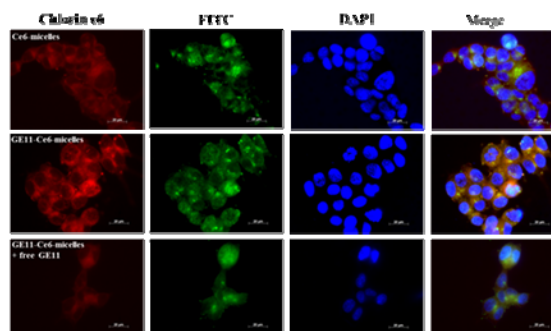


Figure 4: Subcellular localization of chlorin e6 in HCT116 cells treated with EGFR-targeted GE11-Ce6-micelles or non-targeted Ce6-micelles.



The results demonstrated that GE11-Ce6-micelles were effectively accumulated in the HCT116 tumor, compared to non-targeted mixed micelles (Figure 5). At 3 h post-injection, significant fluorescence emitted from the GE11-Ce6-micelles injected mice was observed in the HCT116 tumor but not SW620 tumor.

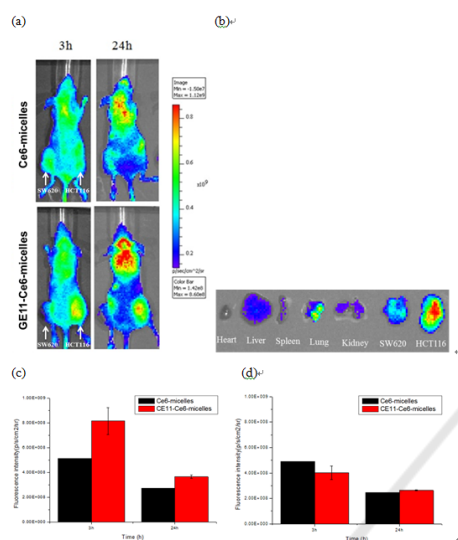


Figure 5: In vivo and ex vivo fluorescence imaging of HCT116 and SW620 tumor-bearing mice administrated with EGFR-targeted GE11-Ce6-micelles and non-targeted Ce6-micelles. (a) Whole body fluorescence images of tumor-bearing mice treated with GE11-Ce6-micelles and Ce6-micelles. Arrows indicate tumor sites. (b) Ex vivo fluorescence images of organs and tumors were acquired after 24 h injection of GE11-Ce6-micelles. The total fluorescent photon counts of chlorin e6 in (c) HCT116 tumor and (d) SW620 tumor in the corresponding fluorescence images in Figure 8a was quantified.

Meanwhile, there are also fluorescence signal in the other tissues. At 24 h post-injection, the fluorescence of GE11-Ce6-micelles was maintained in HCT116 tumor, indicating that it were not subject to rapid excretion from the mice. Additionally, the total fluorescent photon counts of chlorin e6 in tumor with GE11-Ce6-micelles was about 2-2.5 fold higher than that with Ce6-micelles at 3 h and 24h post-injection in HCT116 tumor.

### 3.5 In Vivo Photodynamic Therapy

In vivo photodynamic therapeutic efficacy of GE11-Ce6-micelles or Ce6-micelles (equivalent to 5mg/kg of chlorin e6) with laser irradiation was evaluated by measuring tumor growth in HCT116 tumor-bearing mice. After 24h injection, the tumors were irradiated

with a red laser (670 nm, 634 mW/cm<sup>2</sup>) for 10 min and the tumor size was monitored for 22 days. Figure 6a showed the therapeutic efficacy of each treatment was monitored by evaluating the relative tumor volume for 22 days. The PDT mediated by GE11-Ce6-micelles reduced relative tumor volume compared with control tumors and tumors treated with Ce6-micelles plus laser irradiation. The body weight were not significantly different between control mice and PDT-treated mice, indicating that photodynamic therapy mediated by Ce6-micelles or GE11-Ce6-micelles did not result in unacceptable toxicity (Figure 6b).

## 4 CONCLUSIONS

We have prepared and characterized pH-responsive micelle constructed from graft copolymer PEGMA-co-DPA and diblock copolymer mPEG-b-PCL as drug delivery carrier for simultaneous photodynamic imaging and therapy. In vitro and in vivo studies confirmed that EGFR-targeted o GE11-Ce6-micelles enhanced specific uptake by cancer cells via receptor mediated endocytosis pathway and improved PDT of EGFR overexpressing cancer cells. Moreover, the tumor targeted delivery of GE11-Ce6-micelles allowed detection of EGFR tumors by near infrared imaging. In tumor-bearing mice models, GE11-Ce6-micelles could effectively suppress the tumor growth compared to non-targeted Ce6-micelles. In conclusion, GE11-Ce6-micelles could be successfully applied to fluorescence imaging and effective photodynamic therapy of cancer.

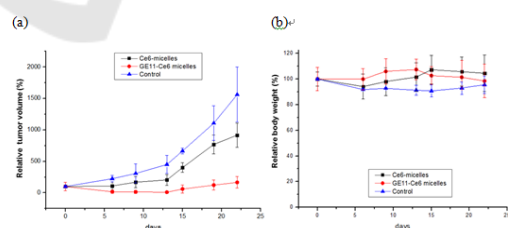


Figure 6: In vivo photodynamic therapeutic efficacy of Ce6-micelles or GE11-Ce6-micelles in HCT116 tumor-bearing mice. (a) The tumor volumes and (b) body weights were measured during the 22-day evaluation period in mice were treated with PBS (Control), Ce6-micelles plus laser irradiation, or GE11-Ce6-micelles plus laser irradiation. Data indicate means and standard errors.

## REFERENCES

- Arteaga, C. L. 2002. Epidermal Growth Factor Receptor Dependence In Human Tumors: More Than Just Expression? *The Oncologist*, 7, 31-39.
- Chaw, C.-S., Chooi, K.-W., Liu, X.-M., Tan, C.-W., Wang, L. & Yang, Y.-Y. 2004. Thermally Responsive Core-Shell Nanoparticles Self-Assembled From Cholesteryl End-Capped And Grafted Polyacrylamides:: Drug Incorporation And In Vitro Release. *Biomaterials*, 25, 4297-4308.
- Huang, P., Xu, C., Lin, J., Wang, C., Wang, X. S., Zhang, C. L., Zhou, X. J., Guo, S. W. & Cui, D. X. 2011. Folic Acid-Conjugated Graphene Oxide Loaded With Photosensitizers For Targeting Photodynamic Therapy. *Theranostics*, 1, 240-250.
- Koo, H., Lee, H., Lee, S., Min, K. H., Kim, M. S., Lee, D. S., Choi, Y., Kwon, I. C., Kim, K. & Jeong, S. Y. 2010. In Vivo Tumor Diagnosis And Photodynamic Therapy Via Tumoral Ph-Responsive Polymeric Micelles. *Chemical Communications*, 46, 5668-5670.
- Lee, P.-C., Chiou, Y.-C., Wong, J.-M., Peng, C.-L. & Shieh, M.-J. 2013. Targeting Colorectal Cancer Cells With Single-Walled Carbon Nanotubes Conjugated To Anticancer Agent Sn-38 And Egfr Antibody. *Biomaterials*, 34, 8756-8765.
- Li, Z., Zhao, R., Wu, X., Sun, Y., Yao, M., Li, J., Xu, Y. & Gu, J. 2005. Identification And Characterization Of A Novel Peptide Ligand Of Epidermal Growth Factor Receptor For Targeted Delivery Of Therapeutics. *The Faseb Journal*, 19, 1978-1985.
- Milane, L., Duan, Z. & Amiji, M. 2010. Development Of Egfr-Targeted Polymer Blend Nanocarriers For Combination Paclitaxel/Lonidamine Delivery To Treat Multi-Drug Resistance In Human Breast And Ovarian Tumor Cells. *Molecular Pharmaceutics*, 8, 185-203.
- Min, K. H., Kim, J.-H., Bae, S. M., Shin, H., Kim, M. S., Park, S., Lee, H., Park, R.-W., Kim, I.-S., Kim, K., Kwon, I. C., Jeong, S. Y. & Lee, D. S. 2010. Tumoral Acidic Ph-Responsive Mpeg-Poly(B-Amino Ester) Polymeric Micelles For Cancer Targeting Therapy. *Journal Of Controlled Release*, 144, 259-266.
- Olivier, J.-C., Huertas, R., Lee, H. J., Calon, F. & Pardridge, W. M. 2002. Synthesis Of Pegylated Immunonanoparticles. *Pharmaceutical Research*, 19, 1137-1143.
- Peng, C.-L., Shieh, M.-J., Tsai, M.-H., Chang, C.-C. & Lai, P.-S. 2008a. Self-Assembled Star-Shaped Chlorin-Core Poly( $\epsilon$ -Caprolactone)-Poly(Ethylene Glycol) Diblock Copolymer Micelles For Dual Chemo-Photodynamic Therapies. *Biomaterials*, 29, 3599-3608.
- Peng, C.-L., Yang, L.-Y., Luo, T.-Y., Lai, P.-S., Yang, S.-J., Lin, W.-J. & Shieh, M.-J. 2010. Development Of Ph Sensitive 2-(Diisopropylamino)Ethyl Methacrylate Based Nanoparticles For Photodynamic Therapy. *Nanotechnology*, 21, 155103.
- Peng, C. L., Lai, P. S., Lin, F. H., Wu, S. Y. H. & Shieh, M. J. 2009. Dual Chemotherapy And Photodynamic Therapy In An Ht-29 Human Colon Cancer Xenograft Model Using Sn-38-Loaded Chlorin-Core Star Block Copolymer Micelles. *Biomaterials*, 30, 3614-3625.
- Peng, C. L., Shieh, M. J., Tsai, M. H., Chang, C. C. & Lai, P. S. 2008b. Self-Assembled Star-Shaped Chlorin-Core Poly(C-Caprolactone)-Poly(Ethylene Glycol) Diblock Copolymer Micelles For Dual Chemo-Photodynamic Therapies. *Biomaterials*, 29, 3599-3608.
- Schmidt-Erfurth, U. & Hasan, T. 2000. Mechanisms Of Action Of Photodynamic Therapy With Verteporfin For The Treatment Of Age-Related Macular Degeneration. *Survey Of Ophthalmology*, 45, 195-214.
- Shen, Y., Tang, H., Radosz, M., Van Kirk, E. & Murdoch, W. 2008. Ph-Responsive Nanoparticles For Cancer Drug Delivery. In: Jain, K. (Ed.) *Drug Delivery Systems*. Humana Press.
- Wang, M., Chen, Z., Zheng, W., Zhu, H., Lu, S., Ma, E., Tu, D., Zhou, S., Huang, M. & Chen, X. 2014a. Lanthanide-Doped Upconversion Nanoparticles Electrostatically Coupled With Photosensitizers For Near-Infrared-Triggered Photodynamic Therapy. *Nanoscale*, 6, 8274-8282.
- Wang, X., Liu, K., Yang, G., Cheng, L., He, L., Liu, Y., Li, Y., Guo, L. & Liu, Z. 2014b. Near-Infrared Light Triggered Photodynamic Therapy In Combination With Gene Therapy Using Upconversion Nanoparticles For Effective Cancer Cell Killing. *Nanoscale*.
- Zhang, G.-D., Harada, A., Nishiyama, N., Jiang, D.-L., Koyama, H., Aida, T. & Kataoka, K. 2003. Polyion Complex Micelles Entrapping Cationic Dendrimer Porphyrin: Effective Photosensitizer For Photodynamic Therapy Of Cancer. *Journal Of Controlled Release*, 93, 141-150.